Supporting Information for "Automated detection and cataloging of global explosive volcanism using the International Monitoring System infrasound network"

Contents of this file

1. Figures S1 to S6 captions
2. Movie M1 caption
3. Figures S1 to S6

Supplementary Figure S1 Caption Data availability at the 41 stations considered between 1 April 2005 and 31 December 2010. Data considered ends at 5 December 2010 for most stations. Green boxes correspond to days during which at least one PMCC family was registered at the station indicated on the vertical axis.

Supplementary Figure S2 Caption Similar to Figures 6–7, but showing expanded azimuth deviation tolerance. In this case, the 2-day "during" grid $\mathbf{G^d}$ is constructed using an azimuth deviation tolerance ψ_{dev} of 5°, while the 10-day "prior" grid $\mathbf{G^p}$ is constructed using an azimuth deviation tolerance of 10°. For illustration in this figure, we set $n^{\text{near}} = 0$. We use $f_{\text{min}} = 0.1$ Hz, $f_{\text{max}} = 5$ Hz, $f_{\text{mean}} = 2$ Hz (as Figure 7), $d_{\text{max}} = 5,000$ km, $v = 0.33$ km/s, and $\alpha = 2.0$ (different to Figures 6 and 7). The grid global maximum is shown by a red circle and the true location of Sarychev Peak by a

magenta triangle. The "masked' grid $\mathbf{G^m}$ shown in (f) represents 3-station detection with an azimuthal gap of 220° at $m = 500$ pixels.

Supplementary Figure S3 Caption Similar to Supplementary Figure S1, but using a more broadband frequency range of $f_{\min} = 0.01$ Hz, $f_{\max} = 5$ Hz, and $f_{\mathrm{mean}} = 5$ Hz as was used for the Kasatochi eruption in Figure 10 of the main text. Here we use an azimuth deviation tolerance ψ_{dev} of 5° and 10° for $\mathbf{G^d}$ and $\mathbf{G^p}$, respectively. For illustration in this figure, we set $n^{\mathrm{near}} = 0$. We set $d_{\max} = 5,000$ km, $v = 0.33$ km/s, and $\alpha = 2.0$. The "masked' grid $\mathbf{G^m}$ shown in (f) represents 3-station detection with an azimuthal gap of 220° at $m = 500$ pixels.

Supplementary Figure S4 Caption Global infrasound catalogs for data from 1 April 2005 to 31 December 2010. Infrasound events are shown as circles colored by the year of occurrence (see legend on right) with symbol size proportional to the number of pixels in the grid $\mathbf{G^m}$ at the detection location (black circles in legend indicate number of pixels). Events represent the global maximum of $\mathbf{G^m}$ in a 2-day time period (only one event is allowed globally during each 2-day time period) (see Section 5). Different results are shown for separate applications of the algorithm with different parameters choices (Runs 1 to 4; see **Table 1**). (b, d, f, h) represent the same catalogs as (a, c, e, g), respectively, but where only events within 250 km of a known GVP volcano [*Siebert and Simkin*, 2002-] are shown. Red inverted triangles show the 41 stations used (**Supplementary Figure S1** shows the temporal availability of data from each station). The number of events in each case is displayed in the title.

Supplementary Figure S5 Caption Same as **Supplementary Figure S4** but for Runs 5 to 8 (see **Table 1**).

Supplementary Figure S6 Caption Same as **Supplementary Figure S4** but for Runs 9 to 12 (see **Table 1**).

Supplementary Movie M1 Caption Animated time-snapshots of a grid $\mathbf{G^d}(\tau_\mathbf{d})$ constructed for the region around Sarychev Peak (yellow circle) during the time 00:00 UTC 11 June to 00:00 UTC 16 June 2009. The time-stamp at the lower left indicates time since 00:00 UTC 11 June 2009. The panel on the left shows 1-hour snapshots (τ_d = 1 hour), while the panel on the right shows the cumulative stack of all previous 1-hour snapshots. The color scale represents the number of pixels in the grid $\mathbf{G^d}$, with blue to red indicating an increasing number of pixels (legends below panels). Neither the correction using prior clutter (eqn. 1) nor the application of additional constraints (eqn. 2) have been performed in this example. This animation illustrates how pixel values in the grid $\mathbf{G^d}$ accumulate with time as more detections are added from all stations. Coastlines are shown by white lines and stations by red inverted triangles (clockwise from top: IS44, IS30, YAG, and IS45; see *Matoza et al.* [2011] for details). The addition of regional station YAG, Republic of Korea enhances the detection capability of this event compared to the IMS network only.

Figure S1: Data availability at the 41 stations considered between 1 April 2005 and 31 December 2010. Data considered ends at 5 December 2010 for most stations. Green boxes correspond to days during which at least one PMCC family was registered at the station indicated on the vertical axis.

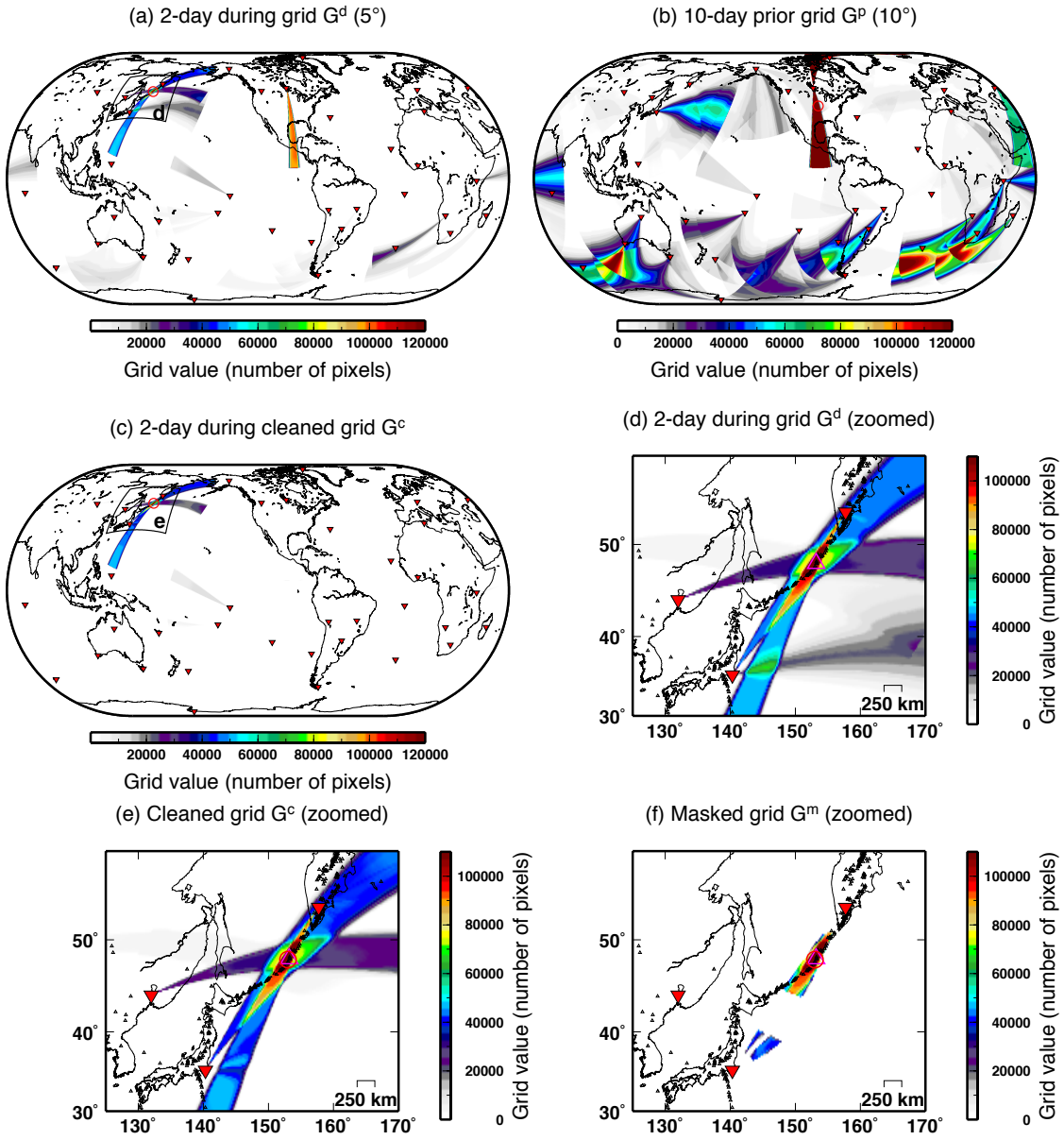

Figure S2: Similar to Figures 5–6, but showing expanded azimuth deviation tolerance. In this case, the 2-day "during" grid $\mathbf{G^d}$ is constructed using an azimuth deviation tolerance ψ_{dev} of 5°, while the 10-day "prior" grid $\mathbf{G^p}$ is constructed using an azimuth deviation tolerance of 10°. For illustration in this figure, we set $n^{\text{near}} = 0$. We use $f_{\text{min}} = 0.1$ Hz, $f_{\text{max}} = 5$ Hz, $f_{\text{mean}} = 2$ Hz (as Figure 6), $d_{\text{max}} = 5,000$ km, $v = 0.33$ km/s, and $\alpha = 2.0$ (different to Figures 5 and 6). The grid global maximum is shown by a red circle and the true location of Sarychev Peak by a magenta triangle. The "masked' grid $\mathbf{G^m}$ shown in (f) represents 3-station detection with an azimuthal gap of 220° at $m = 500$ pixels.

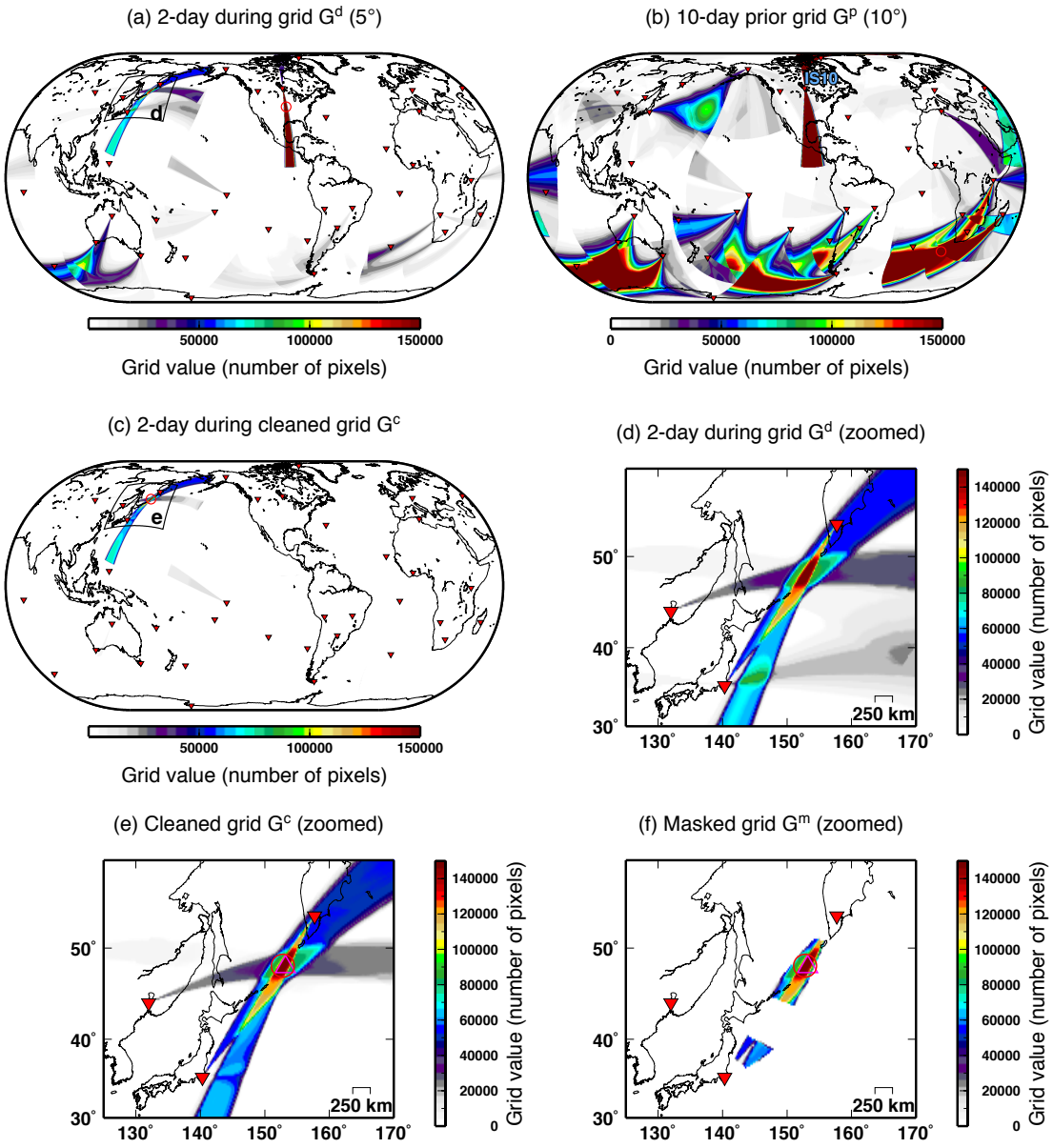

Figure S3: Similar to Supplementary Figure S1, but using a more broadband frequency range of $f_{\min} = 0.01$ Hz, $f_{\max} = 5$ Hz, and $f_{\text{mean}} = 5$ Hz as was used for the Kasatochi eruption in Figure 9 of the main text. Here we use an azimuth deviation tolerance ψ_{dev} of 5° and 10° for $\mathbf{G^d}$ and $\mathbf{G^p}$, respectively. For illustration in this figure, we set $n^{\text{near}} = 0$. We set $d_{\max} = 5,000$ km, $v = 0.33$ km/s, and $\alpha = 2.0$. The "masked' grid $\mathbf{G^m}$ shown in (f) represents 3-station detection with an azimuthal gap of 220° at $m = 500$ pixels.

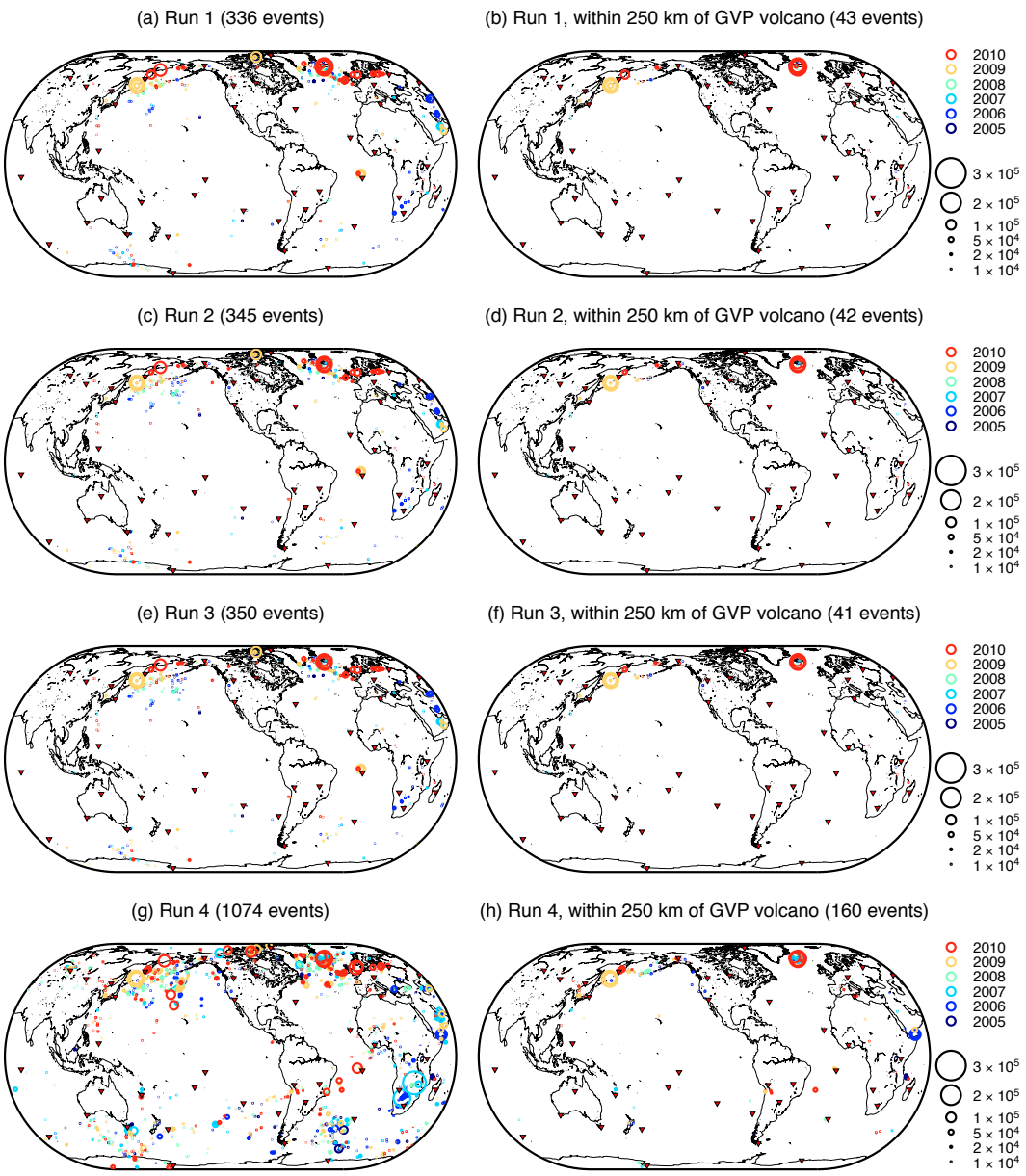

Figure S4: Global infrasound catalogs for data from 1 April 2005 to 31 December 2010. Infrasound events are shown as circles colored by the year of occurrence (see legend on right) with symbol size proportional to the number of pixels in the grid $\mathbf{G^m}$ at the detection location (black circles in legend indicate number of pixels). Events represent the global maximum of $\mathbf{G^m}$ in a 2-day time period (only one event is allowed globally during each 2-day time period) (see Section 5). Different results are shown for separate applications of the algorithm with different parameters choices (Runs 1 to 4; see **Table 1**). (b, d, f, h) represent the same catalogs as (a, c, e, g), respectively, but where only events within 250 km of a known GVP volcano [*Siebert and Simkin*, 2002-] are shown. Red inverted triangles show the 41 stations used (**Supplementary Figure S1** shows the temporal availability of data from each station). The number of events in each case is displayed in the title.

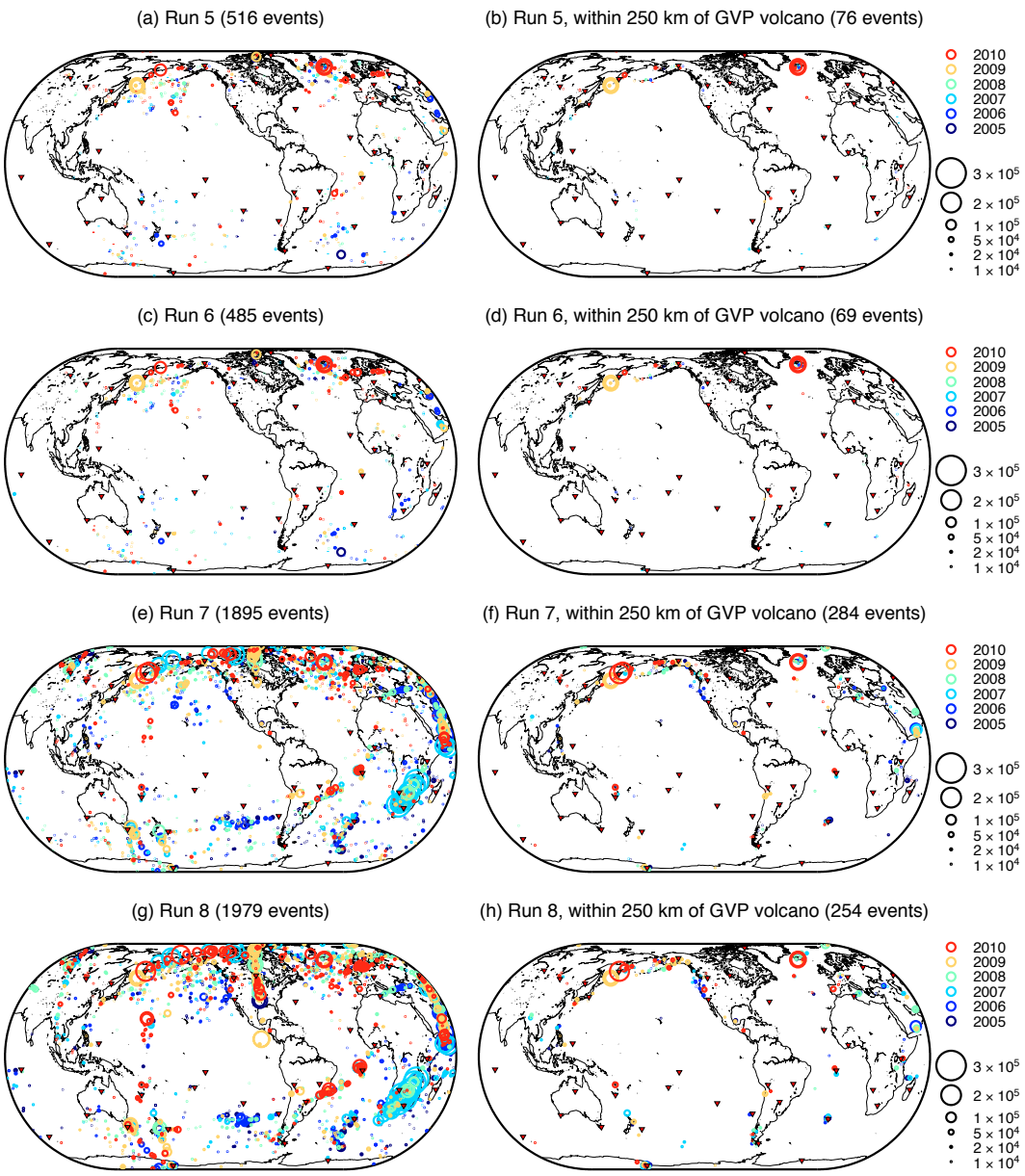

Figure S5: Same as **Supplementary Figure S4** but for Runs 5 to 8 (see **Table 1**).

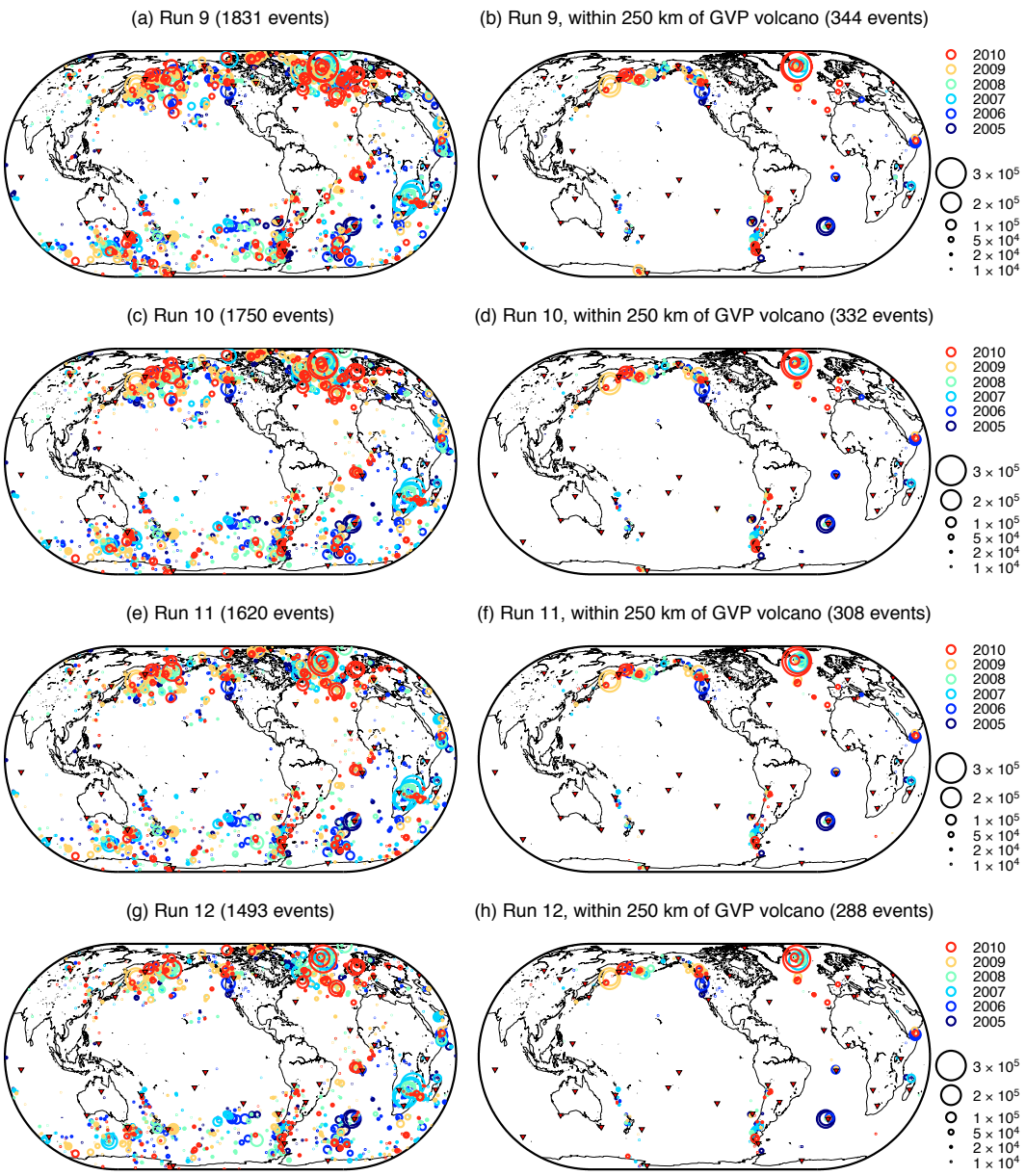

Figure S6: Same as **Supplementary Figure S4** but for Runs 9 to 12 (see **Table 1**).